2005 and involved the development of a database of 90 chemicals on the mouse liver acute response (2, 4, 8, and 24 h after single oral exposure). From 2005 through 2007, an Inhalation Toxicogenomics (ITG) study was added to collect lung transcriptome data at very low exposure levels, near the levels associated with the "sick building" syndrome. From 2006 through 2008, a second stage of the Percellome Project (TTG2) was launched for repeated exposure studies and multi-organ responses studies. Studies of fetus (development) and brain behavior (designated as NTG) were also launched (Affymetrix GeneChip, Mouse Expression 430A, Mouse Genome 430 2.0 Array).

In the TTG1 studies we monitored the time- and dose-dependent gene expressions induced by a single oral administration of a test chemical in mouse liver at four time points (2, 4, 8, and 24 h) and at four dose levels (0, 1×, 3×, 10×), in triplicate (48 per chemical; Figure 15.1). Currently our database contains data for more than 100 chemicals. The data for each 100 chemicals is expressed as a 3-D graph (time × dose × mRNA in copies per cell) made of about 45,000 surfaces corresponding to the probe sets of the Affymetrix MOE430 2.0 GeneChip (see http://www.toxicomics.nihs.go.jp/db/). Two kinds of unsupervise gene clustering methods are developed on the 3-D surface shape. (Aisaki et al., 2007, Matsumoto et al., 2005).

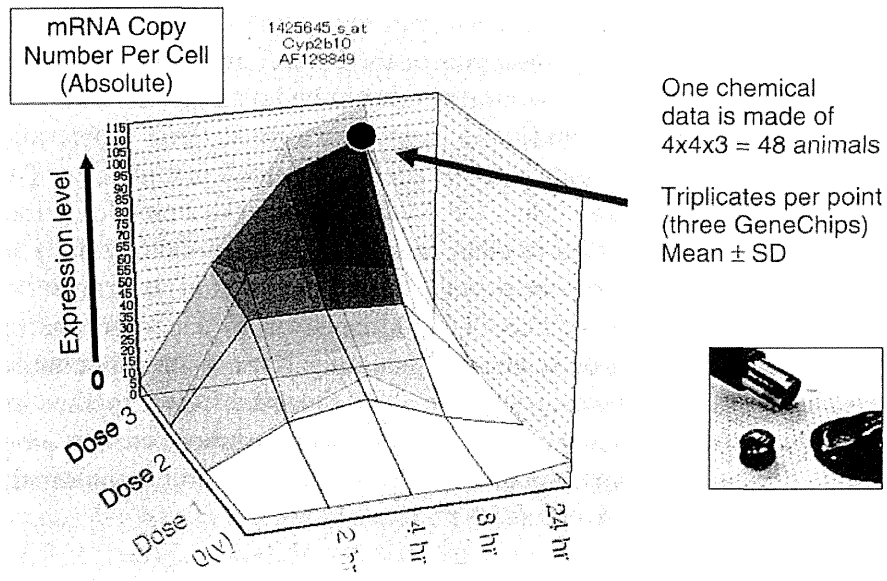

Figure 15.1 Structure of Percellome data showing the surface plot for a single transcript. For mouse liver transcriptome analysis, the mRNA copy numbers per cell of a probe set are plotted on a 4 × 4 (4 time points and 4 dosage levels) matrix to comprise a 3-D graph. One data set of a test chemical consists of about 45,000 layers of 3-D surfaces. Further analysis, such as unsupervised clustering and extraction of significant genes are performed on this 3-D surface data. (*See insert for color representation of the figure.*)

In the TTG2 study, three types of data were generated; the repeated dosing up to 14 days, multiorgan assessments (liver, kidney, lung, heart, testis, brain) after single dosing, and fetus/developmental toxicogenomics (whole embryo, embryonic stem cells, embryoid body). The ITG studies (lung and liver) repeated the dosages for up to 7 days. A series of in-house developed software programs were used and were mostly specified for the 3-D surface data sets to generate time-dependent triggered gene lists and common gene clusters among chemicals. A putative target gene of the knockout phenotypes turned out to completely agree with the estimated effects of the test chemical.

In 2009 a third Percellome Project was launched to comprehensively highlight the toxicity networks from the transcriptomic data collected by the preceding Percellome methods. The additional systems biology approach was incorporated for this purpose. The intention was to keep the transcriptomic data from being biased by the known toxicological information. Without phenotypic anchoring, we attempted to interpret the transcriptomic data by referring to our own transcriptomic database, and genome-based knowledge.

As of 2010 we have compiled a database of more than 100 chemicals, and this database will be available to the public on a "one-chemical one-report" basis. With each report we will include a comprehensive list of genes showing the biologically significant alteration. The home-page for the Percellome database should be available soon.

15.3.1.3 The Japan Microarray Consortium

The Japan Microarray Consortium (JMAC: http://www.jmaqc.org/) has been operating since 2007 and consists of up to seventy of the biochip producing and related companies under the control of the Ministry of Economy, Trade and Industry. This consortium regularly holds working group meetings for the activity of industrial promotion and market creation along with an interest in standardization.

15.3.1.4 The New Energy Development Organization

The New Energy Development Organization (NEDO) had funded a carcinogenesis toxicogenomics project headed by Prof. T. Shirai of Nagoya City University. For up to 28 days, a total of 85 known hepato-carcinogenic, nonhepato-carcinogenic, or noncarcinogenic compounds were given to rats and livers were sampled at days 1, 3, 7, 14, and 28. The gene expression was monitored by in-house microarray (NEDO-ToxArray) and a GeneChip system (RGU34A, Affymetrix). (http://www.nedo.go.jp/iinkai/kenkyuu/bunkakai/18h/jigo/49/1/5-2.pdf, in Japanese).

15.3.1.5 Other Domestic Initiatives

In the domains of clinical medicine, drug development, and chemical/industrial manufacturing, there is broad agreement that comprehensive toxicogenomics data analysis is necessary for the more precise information on the toxicity of ingested chemicals. Yet each sector has been reluctant to make an effort toward the development of a standardization scheme. There are comments that suggest a

desire for concerted action by administrative authorities. The Pharmaceuticals and Medical Devices Agency (PMDA; http://www.pmda.go.jp/english/index.html), which approves new drug applications as commissioned by MHLW, has been holding informal meetings on pharmacogenomics with pharmaceutical companies. In July and October of 2007, PMDA joined the joint FDA/EMEA biomarker validation workshops as an observer. PMDA also asked the Japanese Society of Clinical Pharmacology and Therapeutics to prepare a report on the current status and challenges for pharmacogenomics in drug evaluation (http://www.pmda.go.jp/topics/file/h191113kohyo.pdf, in Japanese). Overall, pharmacogenomics is slowly but steadily moving toward some form of standardization.

15.3.2 International Activities

Major international activities include the MicroArray Quality Control Project (MAQC, US), the External RNA Controls Consortium (ERCC, US), and the European Medicines Agency (EMEA). The MAQC and ERCC bring together scientists from microarray manufacturers, reagent manufacturers, pharmaceutical companies, academia, and government administrative offices. They hold periodic meetings and are rigorously incorporating information from related activities and research. In 2007 they held hearings on the Percellome Project, and the JMAC. MAQC-III has evolved into SEQC (Sequencing Quality Control), and so is charged with the quality control of next-generation high-speed sequencing platforms (http://www.fda.gov/ScienceResearch/BioinformaticsTools/MicroarrayQualityControlProject/default.htm#MAQC-IIIalsoknownasSEQC). At the E15 of the International Conference on Harmonisation of Technical Requirements for Registration of Pharmaceuticals for Human Use (ICH), a *Guidance for Industry; E15 Definitions for Genomic Biomarkers, Pharmacogenomics, Pharmacogenetics, Genomic Data and Sample Coding Categories* was published. This document has set the stage for future contributions to the standardization of terminology in pharmacogenomics. OECD and WHO are also jointly holding toxicogenomics workshops to discuss the future standardization and utilization of toxicogenomics in chemicals safety assessments (http://www.oecd.org/document/29/0,3343,en_2649_34377_34704669_1_1_1_1,00.html and http://www.who.int/ipcs/methods/toxicogenomics/en/).

15.4 CLOSING SUMMARY

The regulatory activities for the standardization of toxicogenomics are progressing rather slowly in Japan. The first area of interest would be the development of toxicopharmacogenomics data for drug approval agencies; it is expected that industrial chemicals would then follow.

The Percellome projects have made all reagents, protocols, and basic analytical tools for quality control available to their collaborators (kanno@nihs.go.jp). The Percellome database will be released to the public sometime in the near future.

ACKNOWLEDGMENT

The authors thank all the members of the Division of Cellular and Molecular Toxicology, NIHS for the support of Percellome Projects and especially Nae Matsuda, Tomoko Ando, Noriko Moriyama, Yuko Kondo, Maki Abe, Koichi Morita, Hisako Aihara and Chiyuri Aoyagi for technical support. This study was supported in part by MHLW Health Sciences Research Grants H19-Iyaku-Ippan-001, H18-Kagaku-Ippan-001, H15-Kagaku-002, and H14-Toxico-001.

REFERENCES

Aisaki, K., Aizawa, S., Fujii, H., Kanno, J., and Kanno, H. (2007). Glycolytic inhibition by mutation of pyruvate kinase gene increases oxidative stress and causes apoptosis of a pyruvate kinase deficient cell line. *Exp Hematol* **35**, 1190–1200.

Kanno, J., Aisaki, K., Igarashi, K., Nakatsu, N., Ono, A., Kodama, Y., and Nagao, T. (2006). "Per cell" normalization method for mRNA measurement by quantitative PCR and microarrays. *BMC Genomics* **7**, 64.

Matsumoto, S., Aisaki, K., and Kanno, J. (2005). Mass distributed clustering: a new algorithm for repeated measurements in gene expression data. *Genome Info* **16**, 183–194.

The Journal of Toxicological Sciences (J. Toxicol. Sci.)
Vol.38, No.4, 643-654, 2013

Original Article

Oral administration of pentachlorophenol induces interferon signaling mRNAs in C57BL/6 male mouse liver

Jun Kanno[1], Ken-ichi Aisaki[1], Katsuhide Igarashi[1], Satoshi Kitajima[1], Nae Matsuda[1], Koichi Morita[1], Masaki Tsuji[1], Noriko Moriyama[1], Yusuke Furukawa[1], Maki Otsuka[1], Erika Tachihara[1], Noriyuki Nakatsu[2] and Yukio Kodama[1]

[1]Division of Cellular and Molecular Toxicology, Biological Safety Research Center, National Institute of Health Sciences, 1-18-1 Kamiyoga, Setagaya-ku, Tokyo 158-8501, Japan
[2]Toxicogenomics Informatics Project, National Institute of Biomedical Innovation, 7-6-8 Asagi Saito Ibaraki-City, Osaka 567-0085, Japan

(Received June 17, 2013; Accepted June 25, 2013)

ABSTRACT — Pentachlorophenol (PCP) was monitored for transcriptome responses in adult mouse liver at 2, 4, 8 and 24 hr after a single oral administration at four dose levels, 0, 10, 30 and 100 mg/kg. The expression data obtained using Affymetrix GeneChip MOE430 2.0 were absolutized by the Percellome method and expressed as three dimensional (3D) surface graphs with axes of time, dose and copy numbers of mRNA per cell. We developed the programs RSort, for comprehensive screening of the 3D surface data and PercellomeExploror for cross-referencing and confirmed the significant responses by visual inspection. In the first 8 hr, approximately 100 probe sets (PSs) related to PXR/SXR and Cyp2a4 and other metabolic enzymes were induced whereas Fos and JunB were suppressed. At 24 hr, about 1,200 PSs were strongly induced. We cross-referenced the Percellome database consisting of 111 chemicals on the liver transcriptome and found that about half of the PSs belonged to the metabolic pathways including Nrf2-mediated oxidative stress response networks shared with some of the 111 chemicals. The other half of the induced genes were interferon signaling network genes (ISG) and their induction was unique to PCP. Toll like receptors and other pattern recognition receptors, interferon regulatory factors and interferon alpha itself were included but inflammatory cytokines were not induced. In summary, these data indicated that functional symptoms of PCP treatment, such as hyperthermia and profuse sweating might be mediated by the ISG rather than the previously documented mitochondrial uncoupling mechanism. PCP might become a hint for developing low molecular weight orally available interferon mimetic drugs following imiquimod and RO4948191 as agonists of toll-like receptor and interferon receptor.

Key words: Pentachlorophenol, Mouse, Liver, Interferon signaling genes, Percellome toxicogenomics

INTRODUCTION

The Percellome Toxicogenomics Project is designed to identify dynamic and extensive networks of genes whose time- and dose-dependent patterns of expression in response to a chemical allows its toxic effects to be predicted. For this project, we developed a standardization method for microarrays and quantitative PCR that produces copy number of mRNAs per one cell (designated as "Percellome method") (Kanno *et al.*, 2006). This method allowed us to directly and quantitatively compare gene expression data among samples, studies, organs and even species using four arithmetic operations. One hundred and eleven chemicals (as of June 2013, Supplementary Table 1), most of which are known for their toxicity, were examined using the standard protocol of the project.

Pentachlorophenol (PCP) was examined in adult male C57BL/6 mouse liver. This compound has been used for multiple purposes such as herbicide, insecticide, fungicide, disinfectant, and other preservative purposes, moreover, its metabolism and toxicity, including carcinogenicity have been well studied. PCP is known to induce morphological changes in liver, kidney, hematopoietic, respiratory, immune and neural systems together with irritation of exposed sites. Hepatocarcinogenicity was demonstrated in rodents; the postulated mechanism involves

Correspondence: Jun Kanno (E-mail: kanno@nihs.go.jp)

hydroxyl radical mediated DNA adduct formation and oxidative stress by the PCP metabolites. Functional symptoms, such as hyperthermia (sometimes life-threatening), profuse sweating, nausea, and uncoordinated movements were noted. Hyperthermia and other functional symptoms have been explained by the uncoupling of oxidative phosphorylation in mitochondria.

Here, we report that a comprehensive Percellome analysis revealed that PCP was the only chemical among the 111 tested in our project that strongly induced the interferon signaling gene (ISG) network. Additional pathways induced by PCP were Nrf2-mediated oxidative stress responses and other metabolic pathways more commonly seem among the 111 chemicals.

MATERIALS AND METHODS

Test chemical

PCP, standard grade (100.0% by gas chromatography coupled with flame ionization detector, Wako Pure Chemical Industries, Ltd., Tokyo, Japan) was dissolved in water containing 0.5% methyl cellulose (Shin-Etsu Chemical Co., Ltd., Tokyo, Japan).

Animal experiments

All experiments were carried out under approval of Experimental Animal Use Committee of National Institute of Health Sciences, Japan. C57BL/6 Cr Slc (Japan SLC, Inc., Shizuoka, Japan) twelve week-old male mice maintained in a barrier system with a 12 hr photoperiod were used in this study. Prior to the main study, a dose finding study was performed. This study revealed that 100 mg/kg was the maximum dose without clinical symptoms or alteration in H&E histology of the liver sampled 24 hr after single oral administration (a standard criteria for the top dose of the Percellome Project study). For the liver transcriptome experiments, forty eight mice were divided into four groups with twelve each, and given a single dose of PCP at 0, 10, 30 and 100 mg/kg by oral gavage. At 2, 4, 8 and 24 hr post-gavage, three randomly selected mice from each dose groups were euthanized by exsanguination under ether anesthesia and the livers were excised into ice-cooled plastic dishes. Tissue blocks weighing 30 to 60 mg were placed in an RNase-free 2 ml plastic tube (Eppendorf GmbH., Hamburg, Germany) and soaked in RNAlater (Ambion Inc., Austin, TX, USA) within 3 min of the beginning of anesthesia. The 12 animal sampling for each time point was finished within 25 to 30 min in order to avoid circadian-based variation within a time point.

Sample preparation and GeneChip measurement

The tissue blocks soaked in RNAlater were kept overnight at 4°C or until use. RNAlater was replaced in the 2 ml plastic tube with 1.0 ml of RLT buffer (Qiagen GmbH., Hilden, Germany), and the tissue was homogenized by adding a 5 mm diameter Zirconium bead (Funakoshi, Tokyo, Japan) and shaking with a MixerMill 300 (Qiagen GmbH) at a speed of 20Hz for 5 min (only the outermost row of the shaker box was used).

Three separate 10μl aliquots were taken from each sample homogenate to another tube and mixed thoroughly. A final 10 μl aliquot there from was treated with DNAse-free RNase A (Nippon Gene Inc., Tokyo, Japan) for 30 min at 37°C, followed by Proteinase K (Roche Diagnostics GmbH., Mannheim, Germany) for 3 hr at 55°C in 1.5 ml capped tubes. The aliquot was transferred to a 96-well black plate. PicoGreen fluorescent dye (Molecular Probes Inc., Eugene, OR, USA) was added to each well, shaken for 10 sec four times and then incubated for 2 min at 30°C. The DNA concentration was measured using a 96 well fluorescence plate reader with excitation at 485 nm and emission at 538 nm. λ phage DNA (PicoGreen Kit, Molecular Probes Inc.) was used as standard.

As reported previously, the graded-dose spike cocktail (GSC) made of the following five *Bacillus subtilis* RNA sequences were selected from the gene list of Affymetrix GeneChip arrays (AFFX-ThrX-3_at, AFFX-LysX-3_at, AFFX-PheX-3_at, AFFX-DapX-3_at, and AFFX-TrpnX-3_at) present in the MOE430 arrays was added to the sample homogenates in proportion to their DNA concentrations (Kanno *et al.*, 2006). Then, the sample homogenates spiked with GSC were processed according to the Affymetrix standard protocol. The GeneChips used were Mouse 430 2.0. We used the in house developed SCal4 (Spike Calculation version 4, by K.A.) to check the efficiency of *in vitro* transcription, and the dose-response linearity of the five GSC spikes and to produce Percellome data, i.e. absolutized mRNA copy numbers of each PS were generated.

The data consist of four dose levels and four time points, generating a 4 x 4 matrix. The mean value (m) with standard deviation (sd) was calculated from the triplicates for all of the probe sets (PSs) for each dose-time points. In order to better visualize the changes at 2 hr, the vehicle value was used for putative zero point, and drawn a 5 x 4 surface three-dimension (3D) surface graph with X-axis for dose, Y for time, and Z for expression as shown in Fig. 1.

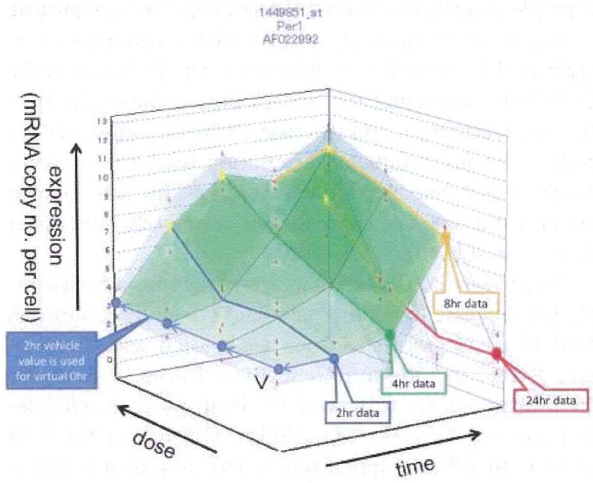

Fig. 1. Three dimensional surface expressions of Percellome Project data: The project data consist of four dose levels and four time points, generating 4 x 4 matrix. The mean value and standard deviation were calculated from the triplicate data. In order to better visualize the changes at 2 hr, the vehicle value was used for zero hour data to draw a 5 x 4 surface graph with X-axis for dose, Y for time, and Z for expression. Here, Affymetrix ID 1449851_at (Per1, period homolog 1) is shown. The 5 x 4 mesh made by the mean values was painted in translucent green (mean surface). The mean surface is rainbow-colored from blue, green, red to yellow according to its peak absolute values (cf. Fig. 3, Supplementary Fig. 1). Above and below the mean surface, +1sd and -1sd surfaces were overlaid using transparent blue. The dose-response curve at 2 hr, 4 hr, 8 hr and 24 hr are highlighted in blue, green, yellow and red. In a direction perpendicular to the dose-response curves, time course of each dose groups and vehicle group is indicated (not highlighted). The graph reads that the highest dose peaked at 4 hr at around 9 copies per cell; the middle dose peaked at 8 hr above 10 copies per cell. The vehicle group (V) showed the circadian change and peaked at 8 hr. The small red crosses are data of each animal sample (n = 3). Yellow asterisks indicate that the marked mean values were significantly different from concurrent vehicle value by $p < 0.05$ (Student's t-test).

Comprehensive selection of treatment-responding mRNAs

The in house developed software, RSort (Roughness Sort by K.A.) was used for automatic selection of treatment-responding mRNAs. This program sorts the PSs based on the roughness of the 3D surface. In other words, calculate the numbers of peaks (upward and downward) in a surface and sort by the number of peaks (maximum of eight peaks in 4 x 4 grid of the surface). Next, it filters the PSs by the number of peaks (normally three or less peaks) and additional parameters such as maximum expression level (normally more than one copy per cell for liver samples), p values between vehicle and top dose groups ($P < 0.05$ or $p < 0.01$). Here, a surface was selected when it had three peaks or less, the first peak in high doses (at any time) or the first peak in middle doses if its value is not significantly different from the neighboring high dose at $p < 0.01$ by Student's t-test, and the value of the peak is significantly different from that of vehicle control at $p < 0.05$ by Student's t-test. These automatically selected PSs were then visually checked for their 3D-surface shapes (to eliminate noisy data), and subdivided into those showed initial changes at 2, 4, 8, and 24 hr. A cross-referencing program named PE (Percellome Explorer, by K.A.) was used to select a list of chemicals that share PSs common to the visually confirmed list of PCP. The PE contains the gene lists automatically selected by the RSort of all data in our Percellome Project (168 datasets for liver samples, 286 for all samples), and automatically cross-refers and sorts out the chemicals sharing the same PSs (Fig. 2). The automatically selected gene lists (product sets) were visually checked to remove noise surfaces.

In Situ Hybridization

For *in situ* hybridization of Irf7 and Stat1 mRNAs, QuantiGeneViewRNA ISH Tissue Assay kit (Affymetrix, Inc., Santa Clara, CA, USA) was used. The probes were designed and synthesized by Affymetrix; regions covered were 2-1461 bases for Irf7 and 707-1710 bases for Stat1. 10% buffered formalin fixed liver tissues were dehydrated and embedded in paraffin. Tissue sections were mounted on "FRONTIER coated glass slides" (Matsunami Glass Ind., Ltd. Osaka, Japan). The slides were completely dried and stored until use. The slides were re-fixed in 10% formaldehyde for 1 hr at room temperature and washed with PBS and deparaffinized with xylene, pretreated in 1x Pretreatment Solution at 98°C for 30 min and digested with Protease QF at 40°C for 20 min. The probes were hybridized at 40°C for 2 hr and the signals were detected with Fast Red.

RESULTS

The numbers of PSs that started to change in response to PCP treatment at 2, 4, 8 and 24 hr were 98, 55, 127 and 1192 respectively (Supplementary Table 2, Supplementary Fig. 1). Chemicals or treatment in the Percellome database (Supplementary Table 1), that shared the PS list with PCP are shown in Table 1. The chemicals that shared the most with the 2 hr PS list of PCP

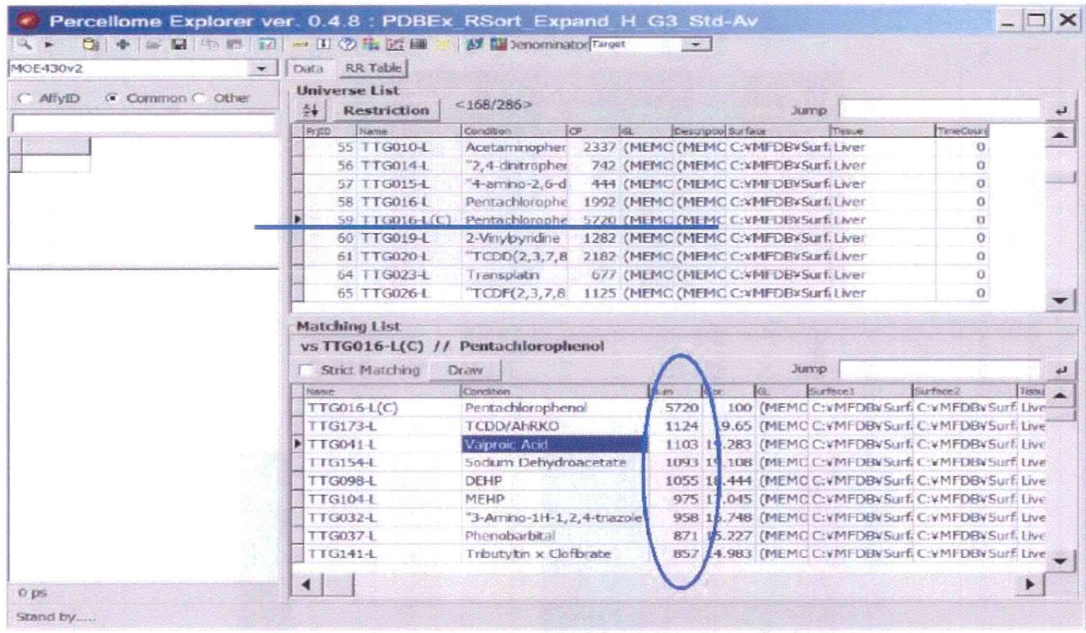

Fig. 2. PercellomeExplorer (PE) Software: The PE contains the gene lists automatically selected by the RSort software program of all data in our Percellome Project (168 datasets for liver samples, 286 for all samples, as of May 2013), and automatically picks up the chemicals sharing same PSs. TTG016-L(C), the study code for PCP was selected from the upper window and the chemicals sharing the PSs were listed in the lower window. These lists await visual confirmation.

was sodium dihydroacetate (TTG154-L); 51 PSs, followed by acephate (TTG109-L); 24 PSs, down to 5-fluorouracil (TTG160-L); 4 PSs. The sum set (or union of sets in set theory) of the 2 hr PS lists that are listed in the 2 hr column of the Table 1 contained 75 PSs (up-regulated (Up) 59, down-regulated (D) 16). Likewise, the sum set of the 4 hr PS lists contained 31 PSs (Up 22, D 9), 8 hr 46 PSs (Up 23, D 23) and 24 hr 636 PSs (all Up). The PS list unique to PCP (Unique list) at each time point contained 23, 24, 81, and 556 PSs at each time points (cf. Supplementary Table 2).

Profiles of genes changed at 2, 4 and 8 hr

The PS list common to other chemicals (Common list) contained the gluconeogenesis pathway of PGC-1A (Ppargc1a)/Foxo1/HNF4 (Puigserver *et al.*, 2003) that were induced at 2 hr (Fig. 3). This finding is in concordance with the report in experimental animals that PCP acutely induces hyperglycemia (Deichman *et al.*, 1942; Clayton and Clayton, 1981). Ppargc1a was reported to increase the expression of Lpin1 (Finck *et al.*, 2006), which was also the case here. A small set of genes encoding metabolic enzymes was induced during the first 8 hr, including Cyp2a4, Cyp4f16, Cyp7a1, Cyp17a1, Cyp39a1, Fmo2, and Fmo5 (Fig. 3).

Ingenuity pathway analysis (Ingenuity Systems, Inc. Redwood City, CA, USA) indicated that these genes are likely to be induced by Nr1i3 (CAR), Nr1i2 (PXR/SXR) or Nr5a1 (data not shown). Although our RSort program did not identify these nuclear receptors, manual search showed that PXR/SXR was induced by PCP (Fig. 3). These changes were not unique to PCP and shared by some of the chemicals in the Common list (cf. Supplementary Table 2).

Down regulation of Fos and JunB at 2, 4, and 8 hr (Fig. 3) was uniquely found in the PCP gene list. Bioinformatic analysis did not identify any associated pathways.

Profiles of genes started to change at 24 hr

The list of PSs induced at 24 hr contained two large networks. About half of the PSs showing altered expression by PCP were assigned to the interferon signaling pathway (Fig. 4, Supplementary Fig. 1). The interferon signaling genes (ISG) were highly up-regulated from Stat1, Stat2, Tyk, to Irf7, Myd88, Oas, Ifit, Cxcl10 and other downstream targets. Toll like receptors (TLRs) and

Table 1. The total numbers of probesets induced by PCP at each time points and those shared with other chemicals.

2 hr			4 hr			8 hr			24 hr		
Percellome No.	Treatment	PS	Percellome No.	Treatment	PS	Percellome No.	Treatment	PS	Percellome No.	Treatment	PS
TTG016-L(C)	Pentachlorophenol	98	TTG016-L(C)	Pentachlorophenol	55	TTG016-L(C)	Pentachlorophenol	127	TTG016-L(C)	Pentachlorophenol	1192
TTG154-L	Sodium Dehydroacetate	51	TTG104-L	MEHP	21	TTG098-L	DEHP	15	TTG098-L	DEHP	258
TTG109-L	Acephate	24	TTG098-L	DEHP	16	TTG041-L	Valproic Acid	14	TTG032-L	3-Amino-1H-1,2,4-triazole	212
TTG059-L	Caffeine	19	TTG037-L	Phenobarbital	14	TTG104-L	MEHP	14	TTG104-L	MEHP	177
TTG062-L(C)	Dexamethasone	18	TTG032-L	3-Amino-1H-1,2,4-triazole	12	TTG109-L	Acephate	13	TTG037-L	Phenobarbital	160
TTG041-L	Valproic Acid	18	TTG144-L	Tributyltin x Phenobarbital	12	TTG160-L	5-fluorouracil	10	TTG041-L	Valproic Acid	109
TTG098-L	DEHP	17	TTG150-L	Valproic acid sodium salt x Thalidomide	8	TTG154-L	Sodium Dehydroacetate	9	TTG157-L	Valproic acid sodium salt	103
TTG019-L	2-Vinylpyridine	15	TTG141-L	Tributyltin x Clofibrate	8	TTG141-L	Tributyltin x Clofibrate	8	TTG031-L	2-Chloro-4,6-dimethylaniline	94
TTG104-L	MEHP	12	TTG074-L	Bromobenzene	8	TTG031-L	2-Chloro-4,6-dimethylaniline	8	TTG154-L	Sodium Dehydroacetate	77
TTG165-L	Chlorpyrifos	12	TTG151-L	Valproic acid sodium salt x Valproic acid sodium salt	7	TTG032-L	3-Amino-1H-1,2,4-triazole	8	TTG162-L	Sesame seed oil unsaponified matter	71
TTG034-L	4-Ethylnitrobenzene	12	TTG031-L	2-Chloro-4,6-dimethylaniline	7	TTG146-L	Forskolin	6	TTG044-L	Clofibrate	69
TTG166-L	Carbaryl	10	TTG044-L	Clofibrate	6	TTG062-L(C)	Dexamethasone	6	TTG074-L	Bromobenzene	47
TTG031-L	2-Chloro-4,6-dimethylaniline	10	TTG162-L	Sesame seed oil unsaponified matter	5	TTG054-L	Diethylnitrosamine (C57BL/6)	5	TTG109-L	Acephate	17
TTG141-L	Tributyltin x Clofibrate	9				TTG132-L	Curcumin	3	TTG160-L	5-fluorouracil	13
TTG032-L	3-Amino-1H-1,2,4-triazole	9				TTG136-L	Phytol	2			
TTG027-L	1,2,3-Triazole	9									
TTG160-L	5-fluorouracil	4									
	Sum Set (common)	75		Sum Set (common)	31		Sum Set (common)	46		Sum Set (common)	636
	Sum Set (Up)	59		Sum Set (Up)	22		Sum Set (Up)	23		Sum Set (Up)	636
	Sum Set (Dn)	16		Sum Set (Dn)	9		Sum Set (Dn)	23		Sum Set (Dn)	0
	PCP NOT Sum (unique to PCP)	23		PCP NOT Sum (unique to PCP)	24		PCP NOT Sum (unique to PCP)	81		PCP NOT Sum (unique to PCP)	556

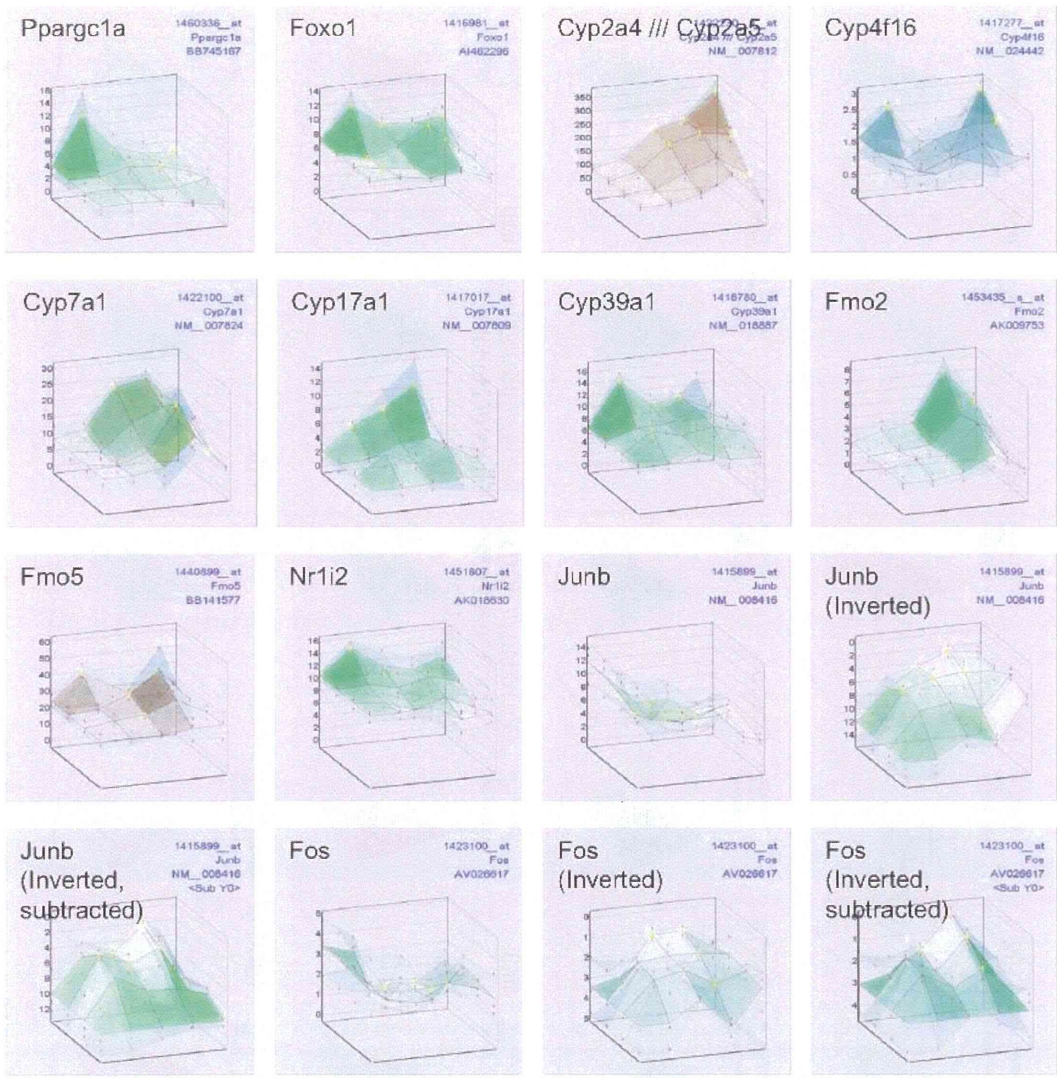

Fig. 3. Representative surface data of PSs induced at 2, 4 and 8 hr after PCP single gavage: Ppargc1a and Foxo1 are the members of gluconeogenesis pathway. A small set of genes of metabolic enzymes, such as Cyp2a4, Cyp4f16, Cyp7a1, Cyp17a1, Cyp39a1, Fmo2, and Fmo5 are induced during the first 8 hr. Nr1i2 or PXR/SXR is also induced. Down regulation of JunB and Fos at 2, 4, and 8 hr are noted. The graphs marked with (Inverted) are plotted with inverted z-axis, zero on top for better indication of suppression. The graphs with (Inverted, subtracted) are plotted, in addition to inverted z-axis, with the 2, 4, 8 and 24 hr values compensated by concurrent vehicle values so that the vehicle line is straight and cancels out the circadian changes.

other pattern recognition receptors (PRR), interferon regulatory factors (Irf) and interferon (Ifn) itself were included. These ISGs were uniquely induced by PCP. It is notable that inflammatory cytokines such as Tnf-α, IL-12 and CD40 were not effectively induced by PCP. The Ingenuity Pathways also plotted many genes in the interferon signaling with a very high probability score (Fig. 6).

In situ hybridization confirmed that hepatocytes were producing the Irf7 and Stat1 in a dose dependent manner (Fig. 7, only vehicle and top dose were shown).

The other half was assigned, by Ingenuity Pathway analysis, to Nrf2-mediated Oxidative Stress Responses

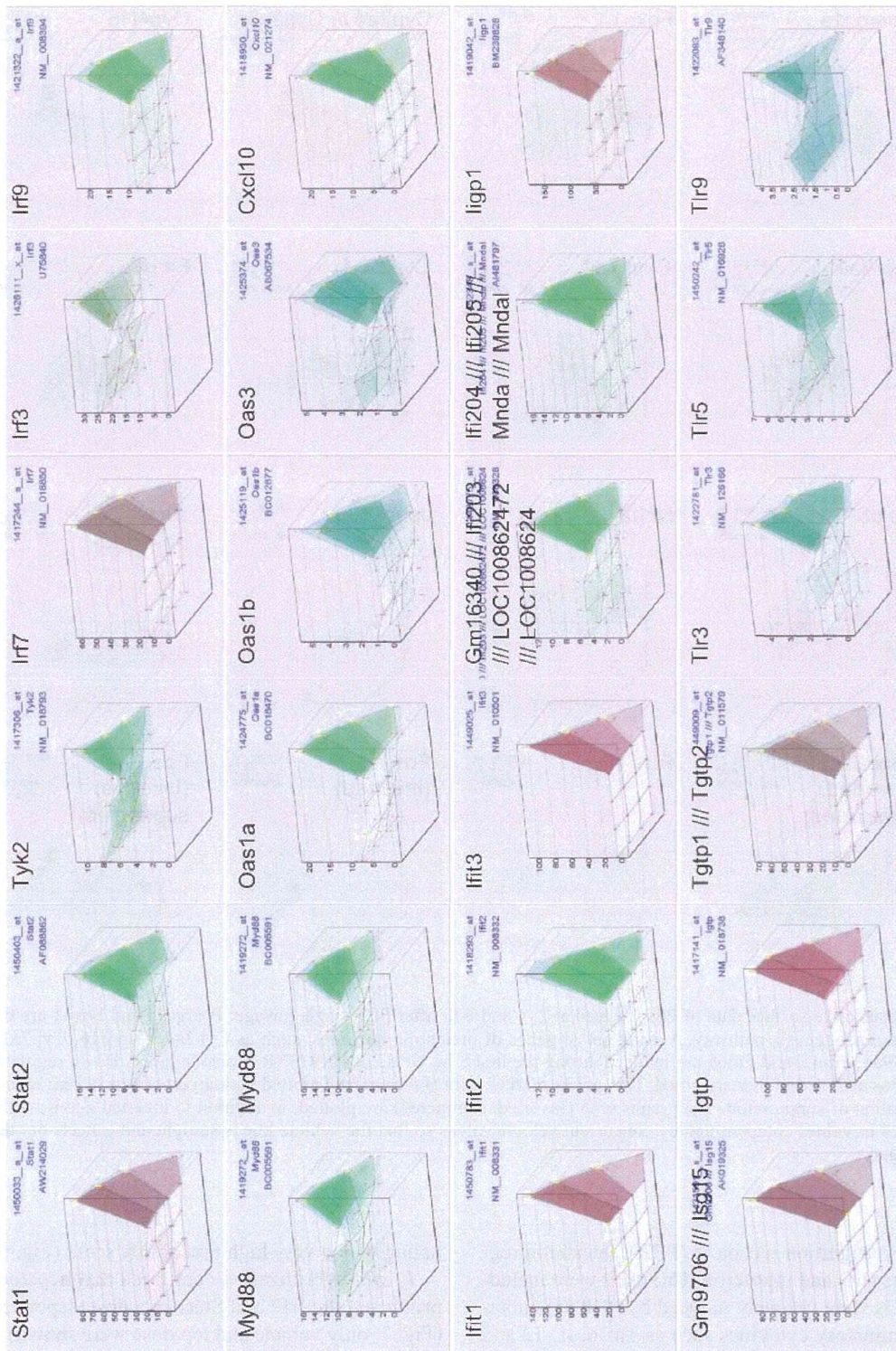

Fig. 4. Surface data of ISGs: Among about 1,200 PSs induced at 24 hr, half of them were uniquely induced by PCP and were assigned to ISG pathway from Stat1, Stat2, Tyk, to Irf7, Myd88, Oas, Ifit, Cxcl10 and other downstream targets. Some Tlrs were also uniquely up-regulated (cf. Supplementary Table 2).

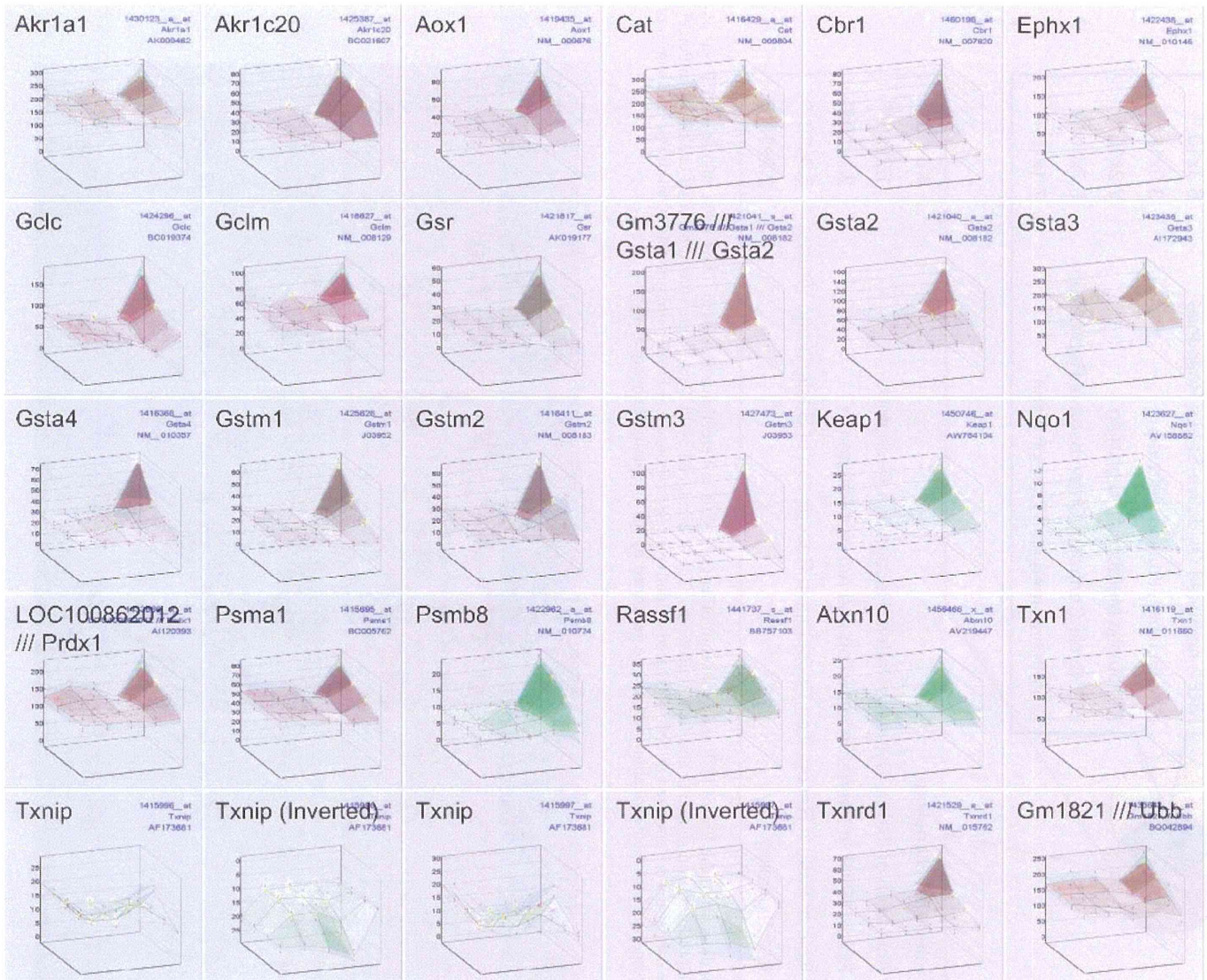

Fig. 5. Surface data of Nrf2-mediated oxidative stress response genes: Among about 1,200 PSs induced at 24 hr, another half of them were Nrf2-mediated oxidative stress response genes commonly induced by PCP and other 10 or so chemicals (cf. Supplementary Table 2). Nrf2 itself did not alter but Keap1 was clearly induced.

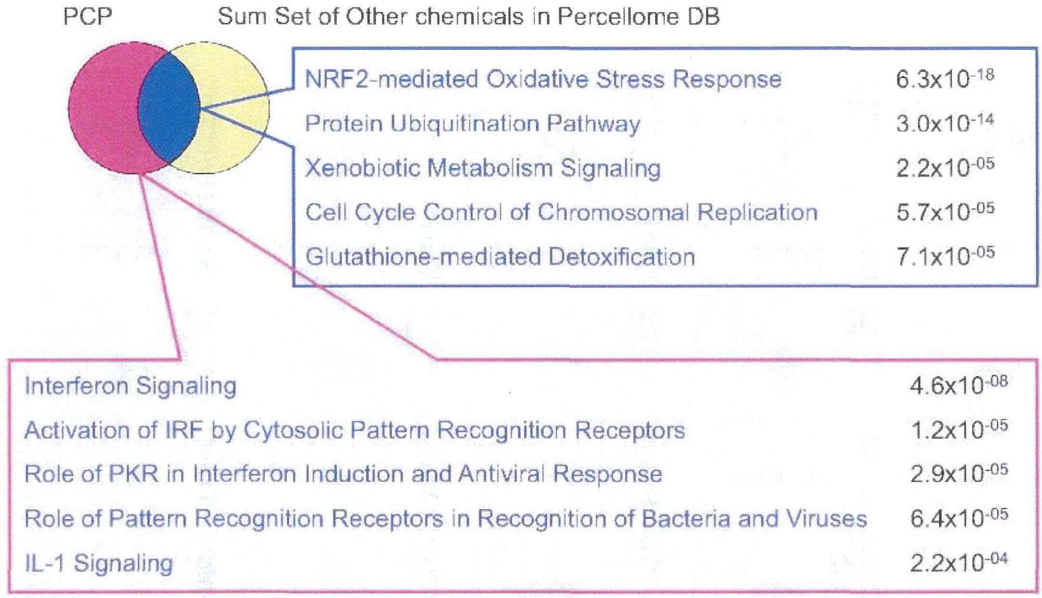

Fig. 6. Venn diagram of the PSs of PCP and sum set of other chemicals in Percellome Database. The PS list unique to PCP was assigned to Interferon signaling and related networks. The PSs induced by PCP and were shared by other chemicals in Percellome database were enriched in Nrf2-mediated oxidative stress response and Protein ubiquitination pathways. The names of the responses and their probability scores are generated by the Ingenuity Pathway analysis.

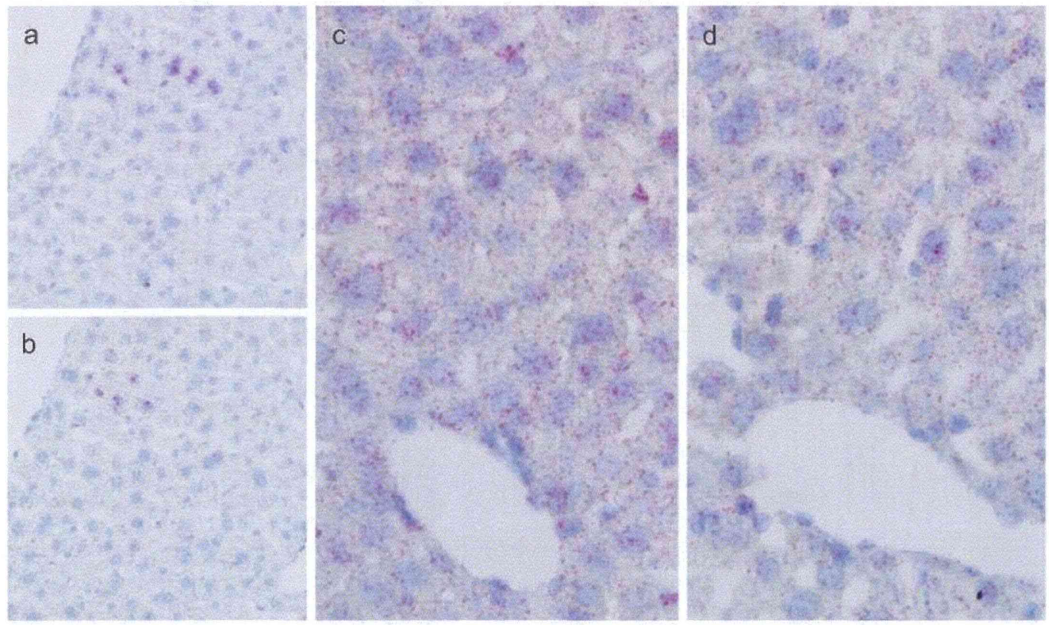

Fig. 7. *In situ* hybridization of Irf7 and Stat1. a) Vehicle control liver stained for Irf7. In a very low back ground, a small nest of hepatocytes was positively stained for Irf7. b) Vehicle control liver stained for Stat1. In a very low back ground, a small nest of hepatocytes was positively stained for Irf7. It is likely that the same hepatocyte is producing both mRNAs. c, d) High dose group stained for Irf7 and Stat1. Hepatocytes were shown to produce both mRNAs in a ubiquitous manner.

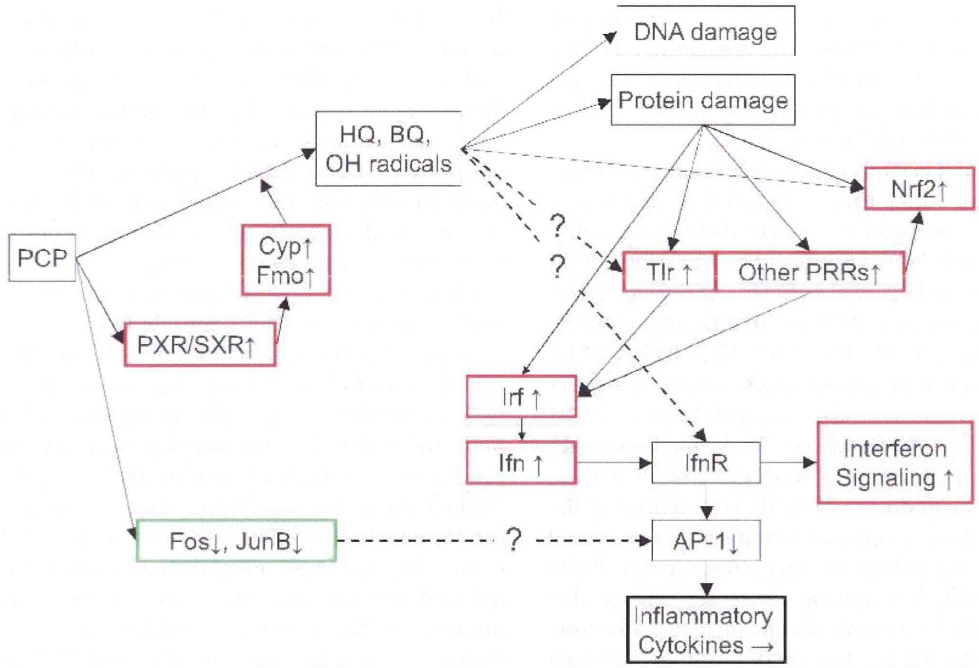

Fig. 8. Tentative summary scheme of the PCP induced networks in mouse liver. PCP or its metabolites may stimulate PXR/SXR or CAR, thereby inducing Cyp2, 4, 7, Fmo2, 5 within 8 hr to facilitate PCP metabolism, generating HQ (TCoHQ,TCpHQ), BQ (TCpBQ) and hydroxyl radical. The metabolites/radicals induce DNA damage and Protein damage. These reaction triggers Nrf2 networks and PRR system, initiating Irf mediated synthesis of Interferon alpha, which triggers the interferon signaling networks by autocrine or paracrine mechanisms. On the other hand, there remains a possibility that the metabolites may act as direct ligands to Tlr or IfnR and trigger downstream events as indicated in dotted lines with "?". Before activating interferon signaling networks, PCP suppressed Fos and JunB, which might have suppressed the inflammatory cytokine induction as shown in dotted line with "?".

accompanying distinct induction of Keap1, and other metabolic pathways (Figs. 5 and 6, Supplementary Table 1). Those networks were in the Common list mentioned above. Other networks were not effectively identified by the Ingenuity pathway analysis.

DISCUSSION

Among the chemicals tested in the Percellome project, PCP was slow to induce changes in gene expression; only around one hundred PSs were induced before 8 hr and 1,200 PSs at 24 hr. It would be plausible to hypothesize that PCP was metabolized during the first 8 hr and that the metabolite(s) then induced the 24 hr burst of ISGs and Nrf2-mediated genes. The time course of PCP action is in accord with the reported biological half-life of PCP; 6 to 27 hr in rodents (Larsen *et al.*, 1972; Braun *et al.*, 1977). A few metabolizing enzymes located downstream of PXR/SXR were induced during the first 8 hr (Fig. 3). The presence of DEHP in the top part of the common chemical list in Table 1 is also consistent with this hypothesis.

It would be of interest to ascertain whether PCP or its metabolite(s) could be PXR/SXR ligands. Metabolites known are tetrachloro-p(o)-hydroquinone (TCpHQ and TCoHQ) and tetrachloro-p-benzoquinone (chloranil, TCpBQ). Further, TCpHQ is reported to be metabolized, generating hydroxyl radicals with a help of H_2O_2 without Fenton reaction, to trichloro-hydroperoxyl-1,4-benzoquinone (TrCBQ-OOH) and trichloro-hydroxy-1,4-benzoquinone (TrCBQ-OH) (Zhu and Shan, 2009). We have no Percellome data of those metabolites and, to date, there are no reports on the interaction of PCP or its metabolites with the PXR/SXR. There are reports that PCP affects the function of estrogen receptor (Jung *et al.*, 2004) and thyroid hormone receptor (Kawaguchi *et al.*, 2008). Further study will be needed to identify the triggering event for the earliest responses to PCP.

Hepatocarcinogenic activity of PCP has been shown by rodent studies (NTP, 1999). The metabolites of PCP mentioned above were considered as the cause of oxidative stress or the hydroxyl radical insults against the liver (Zhu and Shan, 2009; Tasaki *et al.*, 2012).

It was reported that Tlr4-mediated, lipopolysaccharide-induced activation of the Ifn-β promoter was inhibited by PCP in a Myd88-independent way (Ohnishi *et al.*, 2008). On the other hand, PCP was considered to trigger Tlr4 via the induction of hydroxyl radicals (Lucas and Maes, 2013). In our experiment, PCP had significantly up-regulated Myd88, Irak1, Traf6, Tlr2, Tlr3, Tlr5, Tlr9 at 24 hr. Although the induction did not reach statistical significance, Tlr4 expression was also elevated. In addition, Irf 3, Irf7 and Irf9 were also induced. These findings might indicate that the TLR system was triggered by PCP itself, its metabolites or hydroxyl radicals via modifying the cytoplasmic proteins; abnormal proteins might be sensed by the TLRs or the pattern recognition receptors (PRR) system. Since Irf3, 7, 9 and Ifn-α1 expression are also increased, it could be possible that Irf mediated autocrine or paracrine of the Ifn-α is triggered, resulting in a burst of ISGs, as postulated by Sato *et al.* (Sato *et al.*, 2000).

Although Myd88 is mobilized, NF-κB, TNF, IL12 and CD40 were not induced, indicating that there may be a switch towards inflammatory cytokine production that was not directly induced by PCP. In relation to the switching mechanism, there is a report that isopropanol impaired AP-1 activation by removing Fos and JunB from the nuclear region of monocytes *in vitro* and suppressed Tlr4-mediated lipopolysaccharide stimulated Tnf-α production (Carignan *et al.*, 2011). In our data, Fos/JunB was down-regulated at earlier phase. As this change might correspond to AP-1 suppression (Gomard *et al.*, 2010), one possibility could be that PCP itself (as an alcohol/phenol) inhibited inflammatory cytokine production.

In contrast to the possible indirect mechanisms noted above, there are two examples that lead us to consider a possibility of direct activation of the ISGs. The first example is a low-molecular weight compound "imiquimod", a Tlr7 agonist, already on the market for treatment of skin viral infection (Hemmi *et al.*, 2002). Subcutaneous injection of imiquimod was reported to induce fever, sickness behavior and induction of ISG in rats (Damm *et al.*, 2012). The second example is a new polyfluoromethylated compound, 8-(1, 3,4-oxadiazol-2-yl)-2, 4-bis (trifluoromethyl) imidazo [1, 2-a] [1, 8] naphthyridine (RO4948191) which was reported to be an orally available low molecular weight interferon receptor agonist. RO4948191 was shown to induce a set of ISGs (Konishi *et al.*, 2012), such as Oas1, Adar, Bst1, Stat1, Ifit3, Usp18, Isg15, Herc6 and Cxcl10. These two examples of direct ligands to TLR and IFNR lead us to hypothesize that PCP and/or its metabolites may be able to directly activate these receptor systems (Fig. 8). Further investigation will be needed to clarify the molecular mechanism(s) through which PCP administration triggers the ISGs. It is tempting to speculate that this classic toxin, PCP, could be used as a new lead for orally applicable interferon-manipulating and/or cytokine switching drugs.

Hyperthermia or hyperpyrexia, profuse sweating, uncoordinated movement, muscle twitching, and coma are reported in humans and experimental animals as acute symptoms of PCP poisoning. These functional symptoms were reported to be caused by the mitochondrial uncoupling effect of PCP. Ucp2 and Ucp3 and some mitochondrial genes are induced in this study (Supplementary Table 2, Supplementary Fig 1). These genes are supportive for uncoupling effect. However, many of the Krebs cycle enzymes were not induced and those that were induced showed very small increases compared to the induction of ISGs. Some peroxidases were also mildly induced, but catalase was not induced by PCP. In the Percellome database, chemicals reported as uncouplers are aspirin, ethanol, sodium arsenite, and 2,4-dinitrophenol. Under the current computational condition, none of them was picked up as a chemical sharing PS list with PCP.

Taken together, our data may be interpreted to indicate that the functional symptoms represented by hyperthermia can be induced by PCP mainly through the activation of ISGs. This interpretation is backed up by the literature on "endogenous pyrogens" (Dinarello, 1999) and on imiquimod (Damm *et al.*, 2012).

Finally, although not yet perfected, the performance of the RSort and PE programs were demonstrated to be sufficient to sort out biologically meaningful changes for the comprehensive characterization of PCP. Manual searches employing different criteria added about 100 mildly changing PSs (data not shown), but the conclusions of our study were not affected. Nevertheless, further refinement for the better coverage is underway.

In conclusion, the RSort program-based comprehensive cross-reference of the Percellome database revealed that PCP was the only chemical among 111 orally administered chemicals that significantly induced the ISGs in hepatocytes. *In situ* hybridization confirmed that the parenchymal hepatocytes are responding to PCP. Two possible mechanisms were discussed; indirect mechanism via the PRR system, and direct stimulation of the Tlr(s) or IfnR(s). Further study is needed to clarify the possible molecular mechanisms.

ACKNOWLEDGMENTS

The author thanks all the member of the division of Cellular and Molecular Toxicology, NIHS for strong support of the project, and Dr. Bruce Blumberg for critical reading of the manuscript. The project has been supported by MHLW Health Sciences Research Grants H24-Kagaku-Shitei-006, H21-Kagaku-Ippan-001, H19-Toxico-001, H18-Kagaku-Ippan-001, H15-Kagaku-002, H14-Toxico-001, and H13-Seikatsu-012.

REFERENCES

Braun, W.H., Young, J.D., Blau, G.E. and Gehring, P.J. (1977): The pharmacokinetics and metabolism of pentachlorophenol in rats. Toxicol. Appl. Pharmacol., **41**, 395-406.

Carignan, D., Désy, O. and de Campos-Lima, P.O. (2011): The dysregulation of the monocyte/macrophage effector function induced by isopropanol is mediated by the defective activation of distinct members of the AP-1 family of transcription factors. Toxicol. Sci., **125**, 144-156.

Clayton, G.D. and Clayton, F.E. (1981): Toxicology. John Wiley Sons, New York.

Damm, J., Wiegand, F., Harden, L.M., Gerstberger, R., Rummel, C. and Roth, J. (2012): Fever, sickness behavior, and expression of inflammatory genes in the hypothalamus after systemic and localized subcutaneous stimulation of rats with the Toll-like receptor 7 agonist imiquimod. Neuroscience, **201**, 166-183.

Deichman, W., Machle, W., Kitzmiller, K.V. and Thomas, G. (1942): Acute and chronic effects of pentachlorophenol and sodium pentachlorophenate upon experimental animals. J. Pharmacol. Exp. Ther., **76**, 104-117.

Dinarello, C.A. (1999): Cytokines as endogenous pyrogens. J Infect Dis., **179 Suppl. 2**, S294-S304.

Finck, B.N., Gropler, M.C., Chen, Z., Leone, T.C., Croce, M.A., Harris, T.E., Lawrence, J.C.Jr. and Kelly, D.P. (2006): Lipin 1 is an inducible amplifier of the hepatic PGC-1alpha/PPARalpha regulatory pathway. Cell. Metab., **4**, 199-210.

Gomard, T., Michaud, H.A., Tempé, D., Thiolon, K., Pelegrin, M. and Piechaczyk, M. (2010): An NF-kappaB-dependent role for JunB in the induction of proinflammatory cytokines in LPS-activated bone marrow-derived dendritic cells. PLoS One, **5**, e9585.

Hemmi, H., Kaisho, T., Takeuchi, O., Sato, S., Sanjo, H., Hoshino, K., Horiuchi, T., Tomizawa, H., Takeda, K. and Akira, S. (2002): Small anti-viral compounds activate immune cells via the TLR7 MyD88-dependent signaling pathway. Nat. Immunol., **3**, 196-200.

Jung, J., Ishida, K. and Nishihara, T. (2004): Anti-estrogenic activity of fifty chemicals evaluated by in vitro assays. Life Sci., **74**, 3065-3074.

Kanno, J., Aisaki, K., Igarashi, K., Nakatsu, N., Ono, A., Kodama, Y. and Nagao, T. (2006): "Per cell" normalization method for mRNA measurement by quantitative PCR and microarrays. BMC Genomics, **7**, 64.

Kawaguchi, M., Morohoshi, K., Saita, E., Yanagisawa, R., Watanabe, G., Takano, H., Morita, M., Imai, H., Taya, K. and Himi, T. (2008): Developmental exposure to pentachlorophenol affects the expression of thyroid hormone receptor beta1 and synapsin I in brain, resulting in thyroid function vulnerability in rats. Endocrine, **33**, 277-284.

Konishi, H., Okamoto, K., Ohmori, Y., Yoshino, H., Ohmori, H., Ashihara, M., Hirata, Y., Ohta, A., Sakamoto, H., Hada, N., Katsume, A., Kohara, M., Morikawa, K., Tsukuda, T., Shimma, N., Foster, G.R., Alazawi, W., Aoki, Y., Arisawa, M. and Sudoh, M. (2012): An orally available, small-molecule interferon inhibits viral replication. Sci. Rep., **2**, 259.

Larsen, R.V., Kirsch, L.E., Shaw, S.M., Christian, J.E. and Born, G.S. (1972): Excretion and tissue distribution of uniformly labeled 14 C-pentachlorophenol in rats. J. Pharm. Sci., **61**, 2004-2006.

Lucas, K. and Maes, M. (2013): Role of the Toll Like Receptor (TLR) Radical Cycle in Chronic Inflammation: Possible Treatments Targeting the TLR4 Pathway. Mol. Neurobiol., (in press).

NTP (1999): NTP Toxicology and Carcinogenesis Studies of Pentachlorophenol (CAS NO. 87-86-5) in F344/N Rats (Feed Studies). In: Natl Toxicol Program Tech Rep Ser), pp.1-182.

Ohmishi, T., Yoshida, T., Igarashi, A., Muroi, M. and Tanamoto, K. (2008): Effects of possible endocrine disruptors on MyD88-independent TLR4 signaling. FEMS Immunol. Med. Microbiol., **52**, 293-295.

Puigserver, P., Rhee, J., Donovan, J., Walkey, C.J., Yoon, J.C., Oriente, F., Kitamura, Y., Altomonte, J., Dong, H., Accili, D. and Spiegelman, B.M. (2003): Insulin-regulated hepatic gluconeogenesis through FOXO1-PGC-1alpha interaction. Nature, **423**, 550-555.

Sato, M., Suemori, H., Hata, N., Asagiri, M., Ogasawara, K., Nakao, K., Nakaya, T., Katsuki, M., Noguchi, S., Tanaka, N. and Taniguchi, T. (2000): Distinct and essential roles of transcription factors IRF-3 and IRF-7 in response to viruses for IFN-alpha/beta gene induction. Immunity, **13**, 539-548.

Tasaki, M., Kuroiwa, Y., Inoue, T., Hibi, D., Matsushita, K., Ishii, Y., Maruyama, S., Nohmi, T., Nishikawa, A. and Umemura, T. (2012): Oxidative DNA damage and *in vivo* mutagenicity caused by reactive oxygen species generated in the livers of p53-proficient or -deficient gpt delta mice treated with non-genotoxic hepatocarcinogens. J. Appl. Toxicol. DOI: 10.1002/jat.2807.

Zhu, B.Z. and Shan, G.Q. (2009): Potential mechanism for pentachlorophenol-induced carcinogenicity: a novel mechanism for metal-independent production of hydroxyl radicals. Chem. Res. Toxicol., **22**, 969-977.

The web site for GeneChip data

The GeneChip data of PCP are accessible at http://www.nihs.go.jp/tox/TtgPublished.htm

Immunogenetics (2013) 65:107–114
DOI 10.1007/s00251-012-0663-8

ORIGINAL PAPER

MxA transcripts with distinct first exons and modulation of gene expression levels by single-nucleotide polymorphisms in human bronchial epithelial cells

Satoshi Noguchi · Minako Hijikata · Emi Hamano · Ikumi Matsushita · Hideyuki Ito · Jun Ohashi · Takahide Nagase · Naoto Keicho

Received: 3 September 2012 / Accepted: 22 October 2012 / Published online: 18 November 2012

Abstract Myxovirus resistance A (MxA) is a major interferon (IFN)-inducible antiviral protein. Promoter single-nucleotide polymorphisms (SNPs) of MxA near the IFN-stimulated response element (ISRE) have been frequently associated with various viral diseases, including emerging respiratory infections. We investigated the expression profile of MxA transcripts with distinct first exons in human bronchial epithelial cells. For primary culture, the bronchial epithelium was isolated from lung tissues with different genotypes, and total RNA was subjected to real-time reverse transcription polymerase chain reaction. The previously reported MxA transcript (T1) and a recently registered transcript with a distinct 5′ first exon (T0) were identified. IFN-β and polyinosinic–polycytidylic acid induced approximately 100-fold higher expression of the T1 transcript than that of the T0 transcript, which also had a potential ISRE motif near its transcription start site. Even without inducers, the T1 transcript accounted for approximately two thirds of the total expression of MxA, levels of which were significantly associated with its promoter and exon 1 SNPs (rs17000900, rs2071430, and rs464138). Our results suggest that MxA observed in respiratory viral infections is possibly dominated by the T1 transcript and partly influenced by relevant 5′ SNPs.

Keywords Myxovirus resistance A · Single-nucleotide polymorphism · Human bronchial epithelial cells · Transcript variants

Abbreviations

LD	Linkage disequilibrium
HBE	Human bronchial epithelial
ISRE	Interferon-stimulated response element

Introduction

The interferon (IFN) system plays an important role in innate immunity against pathogens. When viral components are detected by pattern recognition receptors, infected cells produce type I (α and β) and type III (λ) IFNs (Randall and Goodbourn 2008). Binding of IFNs to their specific receptors leads to the induction of more than 300 IFN-stimulated genes, including myxovirus resistance A (MxA), also known as the myxovirus (influenza virus) resistance 1, IFN-inducible protein p78 (mouse) (MX1) gene. Following

Electronic supplementary material The online version of this article (doi:10.1007/s00251-012-0663-8) contains supplementary material, which is available to authorized users.

S. Noguchi · M. Hijikata · E. Hamano · I. Matsushita · N. Keicho (✉)
Department of Respiratory Diseases, Research Institute, National Center for Global Health and Medicine, 1-21-1 Toyama, Shinjuku-ku, Tokyo 162-8655, Japan
e-mail: nkeicho-tky@umin.ac.jp

S. Noguchi · E. Hamano · T. Nagase
Department of Respiratory Medicine, University of Tokyo Hospital, Tokyo 113-0033, Japan

H. Ito
Department of Thoracic Surgery, National Center for Global Health and Medicine, Tokyo 162-8655, Japan

J. Ohashi
Molecular and Genetic Epidemiology, Faculty of Medicine, University of Tsukuba, Ibaraki 305-8575, Japan

IFN-induced expression, MxA is thought to form oligomeric rings around the nucleocapsid structures of viruses, thereby inhibiting their transcriptional and replicative functions (Haller and Kochs 2011).

The promoter of the human MxA transcript in the original report contains two IFN-stimulated response elements (ISRE), ISRE1 and ISRE2, near the transcription start site, and both are involved in IFN responsiveness (Ronni et al. 1998). The IFN-stimulated gene factor 3 complex binds to the most proximal ISRE1 and the second ISRE2. ISRE1 is essential for MxA promoter activation, whereas ISRE2 has an enhancing effect in the presence of activated ISRE1 (Ronni et al. 1998). IFN regulatory factor 3 can only bind to ISRE2 for enhancing promoter activation (Holzinger et al. 2007). Around ISRE2, there are two single-nucleotide polymorphisms (SNPs) at nucleotide positions −88 and −123, which confer differences in the promoter activity and binding affinity to nuclear proteins (Hijikata et al. 2001; Ching et al. 2010). Promoter SNPs of MxA are reportedly associated with diseases, including hepatitis C (Hijikata et al. 2000; Hijikata et al. 2001), hepatitis B (Peng et al. 2007), multiple sclerosis (Furuyama et al. 2006), and subacute sclerosing panencephalitis (Torisu et al. 2004). We previously reported the association of MxA promoter SNP with the severity of severe acute respiratory syndrome (SARS; Hamano et al. 2005), and Ching et al. (2010) reported its association with susceptibility to SARS in a larger case–control study. However, the expression levels of MxA have been analyzed only in peripheral blood mononuclear cells (PBMC) or liver cells (Fernandez-Arcas et al. 2004; Kong et al. 2007; Abe et al. 2011; McGilvray et al. 2012).

Because MxA has a pivotal role in host defense against not only SARS coronavirus but also other respiratory viruses such as influenza virus (Haller and Kochs 2011), it is important to characterize the expression profile of MxA in human bronchial epithelial (HBE) cells, a site for replication of many respiratory viruses. In addition, a new transcript variant with alternative 5′ untranslated exons starting 5.5 kb upstream of the original exon 1 has recently been registered in the public database (NM_001144925.1). In the present study, we analyzed the expression patterns of MxA transcripts with distinct first exons. We further investigated the possible effects of their 5′ SNPs on gene expression levels in a panel of primary cultured HBE cells with different genotypes.

Materials and methods

Cell culture

The study protocol was approved by the ethical committee of the National Center for Global Health and Medicine (formerly, International Medical Center of Japan). Primary cultured HBE cells were obtained from the cancer-free bronchi of surgically resected lungs after obtaining written informed consent from the individuals concerned, all of whom were Japanese. HBE cells (n=38) were isolated and cultured as described previously (Gray et al. 1996) and used after three–five passages in this study. In brief, HBE cells were seeded at a density of 5×10^5/well onto collagen-coated six-well Transwell plates (Corning Inc., Corning, NY, USA) and cultured in bronchial epithelial growth medium (BioWhittaker, Walkersville, MD, USA) for 24 h. Thereafter, HBE cells (n=3) were stimulated with 1,000 IU/ml IFN-α (PeproTech EC Ltd., London W6 8LL, UK), 1,000 IU/ml IFN-β (Biosource International, Camarillo, CA, USA), 100 μg/ml polyinosinic–polycytidylic acid [poly(I:C); Sigma-Aldrich, St. Louis, MO, USA], 10 ng/ml IFN-γ (R&D Systems, Minneapolis, MN, USA), 50 ng/ml TNF-α (R&D Systems), 20 μg/ml lipopolysaccharide (LPS; Sigma-Aldrich), 10 μg/ml α-defensin 1 (Peptide Institute Inc., Osaka, Japan), 10 μg/ml β-defensin 1 (Peptide Institute Inc.), and 10 μg/ml β-defensin 2 (Peptide Institute Inc.) for 24 h and then harvested. Unstimulated HBE cells (n=38) and those stimulated with 100 μg/ml poly(I:C) for 24 h (n=29) or with 1,000 IU/ml IFN-β for 12 h (n=9) were harvested, and gene expression levels were then analyzed. To assess time-dependent changes in mRNA expression, BEAS-2B cells (ATCC number CRL-9609) were stimulated with 100 μg/ml poly(I:C) for 6, 12, 24, and 48 h.

Real-time reverse transcription polymerase chain reaction

We designated the MxA transcript originally reported by Horisberger et al. (1990) (NM_002462.3) as the T1 transcript and the new transcript variant in the public database (NM_001144925.1) as the T0 transcript. Distinct exons used in the T0 transcript are shown as exons 0a, 0b, and 0c (Fig. 1). Translational start codons of both the T1 and T0 transcripts originate from exon 5, indicating that exons 0a–0c and exons 1–4 are all 5′ untranslated exons.

Total RNA of the cells was extracted using the RNeasy Mini Kit (Qiagen, Hamburg, Germany). Human Total RNA Master panel II (Clontech, Mountain View, CA, USA) was used to investigate gene expression in various tissue types. Most of the tissue RNA in this panel consisted of pooled RNA from two or more donors, and their genotypes were not available. One microgram of total RNA was subjected to RT with random nonamers using SuperScript III Reverse Transcriptase (Invitrogen, Carlsbad, CA, USA). MxA mRNA expression was analyzed by real-time reverse transcription polymerase chain reaction (RT-PCR) using SYBR Premix Ex Taq (Takara Bio, Shiga, Japan) and CFX96 (BioRad, Hercules, CA, USA). Sense and antisense primers were located in exons 0b and 0c (5′-CCAGAGCAACTCCACACCGGGTGC-3′ and 5′-GCTATGGTTCCAATCCAGGTGATC-3′) for the T0 transcript and exons 1 and 2

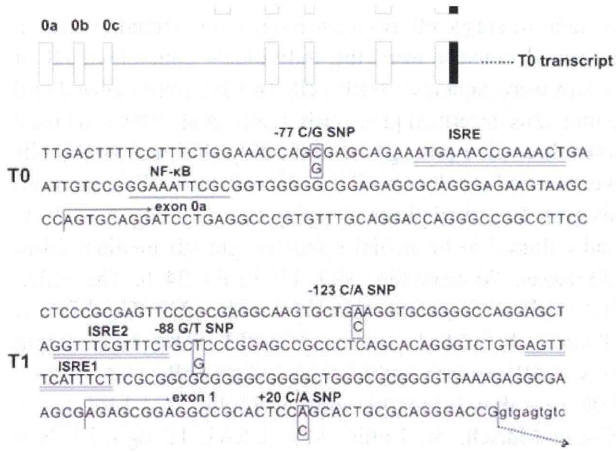

Fig. 1 Alternate splicing of 5′ exons in MxA. The 5′ genomic structure of MxA and nucleotide sequences around the transcription start sites of the T0 and T1 transcripts are shown. *White boxes* represent the untranslated mRNA sequence, and *black boxes* represent the translated sequence. Potential ISREs are *double underlined*, NF-κB binding site is *underlined*, and promoter and exon 1 SNPs are *boxed*. The transcription start site (Horisberger et al. 1990) and nucleotide positions shown in the T1 transcript are displayed in accordance with MxA promoter analysis by Ronni et al. (1998)

(5′-GCACTGCGCAGGGACCG-3′ and 5′-TGGG-TGAG-CAGGTGGGCGGCA-3′) for the T1 transcript. PCR conditions consisted of 40 cycles of denaturation for 15 s at 95 °C and annealing and extension for 1 min at 60 °C. Specific target amplification was confirmed by a single peak in the dissociation curve. The mRNA copy numbers between different transcripts were compared using the absolute quantification method (Leong et al. 2007). RT-PCR products were purified using the Wizard PCR Preps DNA Purification System (Promega, Fitchburg, WI, USA), and their copy numbers were calculated from the DNA concentration determined by measuring the absorbance at 260 nm. The standard curve was generated with a serial fivefold dilution of each RT-PCR product, and the linear dependence of the threshold cycles was confirmed from the template concentrations. We used the β-actin gene (primers listed in Online Resource 1) to normalize the expression of MxA for calculating the relative amounts of mRNA of each transcript. The TaqMan Gene Expression Assay (Hs00182073_m1) (Applied Biosystems, Foster City, CA, USA) that amplifies exons 16–17 of MxA was used with TaqMan Universal Master Mix II (Applied Biosystems) in the StepOne Plus Real-Time PCR System (Applied Biosystems), and the relative amount of total transcripts, indicating the overall expression of MxA, was calculated using the standard curve method with glyceraldehyde 3-phosphate dehydrogenase as an internal control.

Rapid amplification of 5′ cDNA end

RNA ligase-mediated rapid amplification of 5′ cDNA end (5′ RACE) was performed using total RNA from IFN-β-stimulated HBE cells to determine the transcription start site of T0 using the First-Choice RLM-RACE Kit (Ambion, Austin, TX, USA). Gene-specific primers are listed in Online Resource 1. PCR products were sequenced with the BigDye Terminator v3.1 Cycle Sequencing Kit (Applied Biosystems) using a 3130xl Genetic Analyzer (Applied Biosystems).

Screening and genotyping of polymorphisms in the 5′ region

Genomic DNA was extracted from HBE cells (n=38) using the QIAamp DNA Mini Kit (Qiagen). The 5′ upstream region of the transcription start site for the T0 transcript was amplified with two overlapping PCR products, and the amplified products were sequenced using appropriate inner primers. Three SNPs, −123 C/A (rs17000900), −88 G/T (rs2071430), and +20 C/A (rs464138), two in the promoter and one in exon 1 of the T1 transcript, were genotyped by PCR and restriction fragment length polymorphism methods (Hamano et al. 2005), with Pst I (Takara Bio) for rs17000900, Hha I (Takara Bio) for rs2071430, and Bpm I (New England Biolabs, Ipswich, MA, USA) for rs464138. The primers are listed in Online Resource 1. Linkage disequilibrium (LD) between promoter SNPs was analyzed using Haploview (v. 4.2) (Barrett et al. 2005).

Statistical analysis

All data were expressed as mean±standard error of the mean (SEM). To assess the relationship between the number of single alleles of −123 C/A, −88 G/T, and −20 C/A SNPs and expression levels of the transcript variants, a simple linear regression model was applied (JMP, version 9.0.0; SAS Institute Inc., Cary, NC, USA). A multiple linear regression model was also applied to assess the combined effects of these SNPs on expression of the T1 transcript. The numbers of alleles of the three abovementioned SNPs were incorporated in the model as explanatory variables. Correlations of the total amount of the MxA transcripts with expression levels of the T0 and T1 transcripts were further analyzed using Spearman's rank correlation coefficient. A p value <0.05 was considered to be statistically significant.

Results

Expression patterns of MxA transcripts in human tissues

The originally reported MxA transcript, T1, and a recently registered transcript variant, T0, were both successfully

amplified by RT-PCR from various human tissues (Fig. 2). Expression of the T1 transcript was predominant in the tissues examined, including the lung and trachea, whereas expression of the T0 transcript was inconspicuous, except in the testis and adrenal gland.

Induction patterns of MxA transcripts in HBE cells incubated with type I IFNs and other stimuli

MxA transcripts, T0 and T1, were both detected in the unstimulated primary cultured HBE cells ($n=3$), and their expression was markedly induced by type I IFNs and poly(I:C), although induction of the T1 transcript was much stronger than that of the T0 transcript (Fig. 3). IFN-γ, TNF-α, and α-defensin 1 also induced expression of the T1 transcript to a lesser extent, whereas this increase was not observed in the T0 transcript.

Genomic structure and genetic polymorphisms in the 5′ upstream regions of MxA transcripts with distinct first exons

Because the transcript variant T0 with alternatively spliced exons was moderately induced by type I IFNs, 5′ RACE was performed to determine the 5′ end of exon 0a, the transcription start site of T0, in IFN-β-stimulated HBE cells (Fig. 1). A putative ISRE motif and a possible binding site for NF-κB were revealed in the 5′ upstream region of the T0 transcript (Fig. 1). The nearly full-length transcript T0 was amplified with the sense primer in exon 0c and the antisense primer in the last exon 17; however, no alternatively spliced exon was observed in the protein-coding region (data not shown). Although the transcript variant that skips untranslated exons 2 and 4 has also been registered in the public database (NM_001178046.1), its expression level was very low in the HBE cells (data not shown).

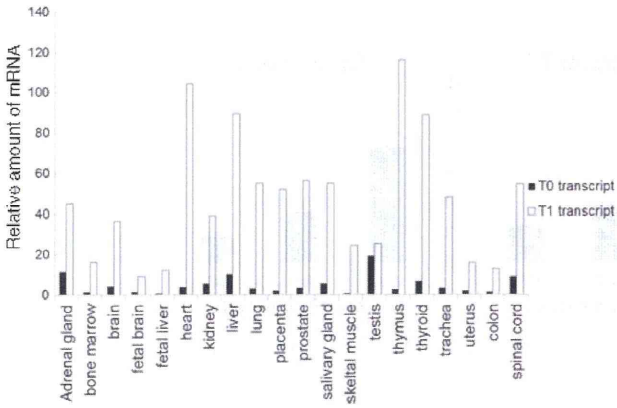

Fig. 2 Relative expression levels of two MxA transcript variants in human tissues. Relative expression levels of the T0 and T1 transcripts in various human tissues were obtained by real-time RT-PCR using a commercial RNA panel, Human Total RNA Master panel II (Clontech). The RNA consisted of pooled RNA from two or more donors. Their genotypes were not available but presumably mixture of different genotypes

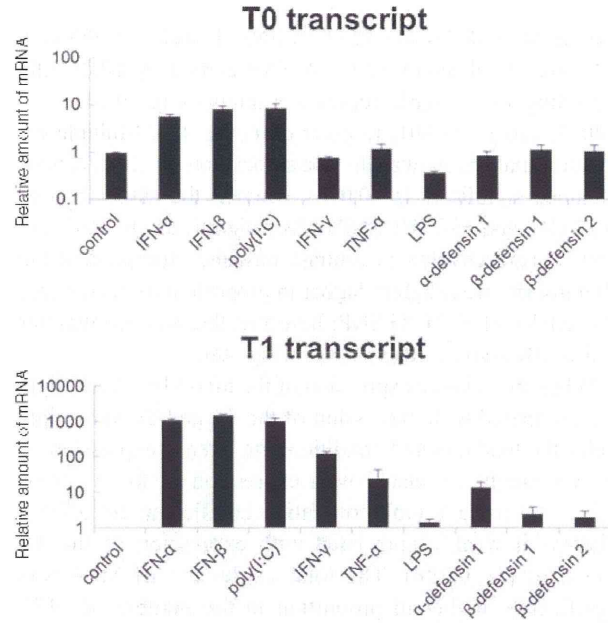

Fig. 3 Induction of T0 and T1 transcript variants by various stimuli in HBE cells. HBE cells ($n=3$) were stimulated with IFN-α, IFN-β, poly (I:C), IFN-γ, TNF-α, LPS, α-defensin 1, β-defensin 1, and β-defensin 2 for 24 h and then harvested. Expression levels of the T0 and T1 transcripts were compared with those of unstimulated cells by real-time RT-PCR. Fold inductions are shown as the mean ± SEM. The genotypes of the promoter SNPs were as follows: sample #1, −77 SNP (rs457274) C/G, −123 SNP (rs17000900) C/A, −88 SNP (rs2071430) G/T, and −120 SNP (rs464138) C/A; sample #2, −77 C/C, −123 C/A, −88 T/T, and +20 A/A and; sample #3, −77 C/G, −123 C/C, −88 G/G, and +20 C/A

Sequence analysis of the 5′ upstream region of the T0 transcript using our DNA samples identified genomic variations, −77 C/G SNP (rs457274) near the putative ISRE motif (Fig. 1), −326 deletion/insertion polymorphism (rs60467231), and −504 A/G SNP (rs12483338). Three other SNPs, −123 C/A (rs17000900), −88 G/T (rs2071430), and −20 C/A (rs464138), near the 5′ end of the T1 transcript were also detected (Fig. 1). As shown in Online Resource 2, −77 C/G SNP of the T0 transcript and the three SNPs near the 5′ end of the T1 transcript were all in strong LD with each other ($D'>0.8$, $r^2>0.4$).

Differences in expression levels of MxA among SNP genotypes

Next, the mRNA expression levels of the T0 and T1 transcripts were analyzed in HBE cells with different genotypes. The expression of the T1 transcript assessed by real-time RT-PCR was 2.3-fold higher than that of the T0 transcript under the unstimulated condition ($n=38$). Baseline expression of the T1 transcript was significantly higher in proportion to the